

Original Article

DOI 10.1007/s12206-022-0128-4

Keywords:

- Least squares method
- Model calibration
- Model error
- Sensitivity

Correspondence to:

Sanghoon Lee  
shlee1222@kmu.ac.kr

Citation:

Lee, G., Lee, S., Kim, N. (2022). A study on model calibration using sensitivity based least squares method. *Journal of Mechanical Science and Technology* 36 (2) (2022) 809–815.  
<http://doi.org/10.1007/s12206-022-0128-4>

Received July 7th, 2021

Revised September 24th, 2021

Accepted October 12th, 2021

† Recommended by Editor  
Hyun-Gyu Kim

# A study on model calibration using sensitivity based least squares method

Gwangtaeck Lee<sup>1</sup>, Sanghoon Lee<sup>1</sup> and Namho Kim<sup>2</sup>

<sup>1</sup>Department of Mechanical and Automotive Engineering, Keimyung University, Daegu 42601, Korea,

<sup>2</sup>Department of Mechanical and Aerospace Engineering, University of Florida, Gainesville, FL 32611, U.S.

**Abstract** In the field of engineering, simulations are often used to save experimental cost and time. Since most of the simulation models have various model errors, the simulation results may differ from the actual one. It is important to accurately calibrate and predict parameters as the calibrated parameters can be applied to other simulations and are used as important design criteria. Therefore, if there is an error in the simulation model, this model error should be taken into consideration when parameters are calibrated. The calibration method usually uses a function value based least squares method, but when there is an error in the simulation model, it fits well at the training point, but an error may occur at the prediction point. For this reason, Qiu et al. [1] proposed a sensitivity based the least squares method—a method of calibrating model parameters by matching the slope of the simulation result and the slope of the actual value. In this paper, the performance and applicability of SLS is further investigated with two examples. In the cantilever beam example which was studied earlier by Qiu et al. [1], a finite element model is introduced to account for various sources of error. In the open hole tension test example, the performance of SLS in a multidimensional problem was examined and compared with FLS.

## 1. Introduction

With the advance of computers, computer-aided engineering (CAE) is being used in various engineering applications such as automobiles, aircraft, and architecture to reduce experimental costs and time [2-4]. At the same time, concerns about the reliability of the CAE models are increasing. Thus, there has been a growing interest in improving and proving the reliability of the CAE model [5-7].

Since most simulation models have various sources of errors, such as numerical error, the results of the simulation models often differ from those of physical experiments which also contain measurement errors. Thus, when the simulation model has a model discrepancy, it is important to take into account this discrepancy when calibrating the model parameters. If the model discrepancy is not considered, calibration and validation of model parameters may not be performed properly even if the amount of data is increased. Loepky et al. [8] pointed out that the exact value of the parameter can be obtained only when the model discrepancy is properly considered.

Most studies have focused only on the results at training points where the actual and simulation values are matched and do not focus on the accuracy of the validation points predicted by the calibrated parameters [9]. However, since the calibrated parameter can be applied to other simulations and used as an important design criterion, it is important to accurately calibrate and predict the parameter considering the entire design space [10]. The existing parameter calibration method uses a function value based least squares method (FLS), which is a method of determining model parameters by minimizing the error between the simulation result and the actual value. However, if there is a model discrepancy in the simulation model, even if the simulation result and the actual value fit well at the training points, a large error may occur at the validation points.

Recent calibration and validation methods include a statistical approach using the Bayesian

method [1]. Kennedy et al. [9] proposed a Bayesian calibration framework that includes various discrepancies and showed that errors can be reduced or mitigated when calibrating parameters by introducing discrepancy functions. Mahadevan et al. [5, 11] discussed the effects of different model discrepancies and showed their effect on the calibration results. However, the statistical approach requires knowledge of statistical theory and a large number of experimental and simulation data [1]. This is not an easy task for industrial applications. For this reason, Qiu et al. [1] proposed a simpler sensitivity based least squares method (SLS) for practical applications. The SLS uses sensitivity instead of statistical measures, and uses a simple form of discrepancy function to be minimized for parameter calibration. It is a method of minimizing errors while following the trend of the actual model by matching the slope of the simulation result with that of the actual value.

In this paper, the performance and applicability of SLS is investigated in comparison with the conventional FLS. The cantilever beam example dealt in Qiu et al. [1] is revisited. Instead of analytic model given in mathematical equations, a finite element model of beam is constructed of which the material parameters are calibrated with FLS and SLS to account for more practical model errors. A new example of a composite plate with an open hole under tensile test was investigated to check the performance of SLS in a multi-dimensional problem.

Sec. 2 of this paper introduces the FLS and the SLS and the two examples mentioned above follow in Secs. 3 and 4.

## 2. Model calibration methods

### 2.1 Function value based least squares method

This section introduces two calibration methods. The first calibration method is the FLS. In general, both the measurement data and prediction have errors. To simplify the presentation, it is assumed that there is no measurement error, that is, the measurement data are actual values. Then, the relationship between prediction and measurement can be written as

$$y_{test}(d) = y_{pre}(d, \theta) + e \quad (1)$$

where  $d$  is the control parameter in the design space and  $\theta$  is the calibration parameter. And  $e$  is the error between the predicted value  $y_{pre}$  of the calibrated model and the actual value  $y_{test}$ .

When more than one data is used, the value of the calibration parameter is determined by minimizing the sum of squared errors using Eq. (2) [12].

$$\min_{\theta} \sum_{i=1}^N w_i [y_{test,i}(d) - y_{pre,i}(d, \theta)]^2 \quad (2)$$

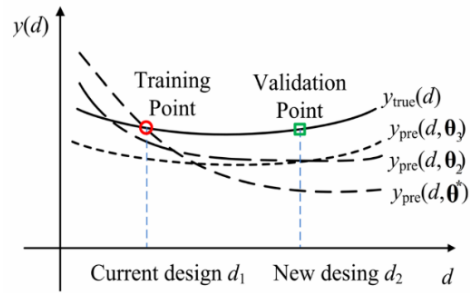


Fig. 1. Schematic of model calibration and model validation [1].

where  $w_i$  is the weight of the  $i$ -th measurement, which represents the confidence level of the measurement. In this study, since no preference is given to a specific measurement, a constant weight is used for all measurements.  $N$  is the number of data used for the least squares method.

The optimal parameter  $\theta^*$  from Eq. (2) can be used to predict the function at untested design  $y_{pre}(d, \theta^*)$ . However, as shown in Fig. 1, the parameter  $\theta^*$  can cause a large error at prediction points if there is a discrepancy in the model [1]. In this case, the calibration accuracy may not be improved even though more data points are taken for calibration.

### 2.2 Sensitivity based least squares method

The second calibration method is the SLS. In general, the shape of the model discrepancy is not known; however, it should be taken into consideration at least as a simple constant function. The  $e_{model}$ ,  $e_{num}$ , and  $e_{test}$  in Eq. (3) are modeling error, numerical error, and measurement error, respectively. Their sum  $\delta$  is used to account for the discrepancy. Even if the actual model discrepancy may not be constant, better calibration results can be obtained than the conventional method, FLS, by assuming a constant model error and reflecting it in the model calibration.

$$y_{test}(d) = y_{pre}(d, \theta^*) + e_{model} + e_{num} - e_{test} = y_{pre}(d, \theta^*) + \delta \quad (3)$$

In SLS, the discrepancy is removed by subtracting the functions at two different designs, which represents the sensitivity of the function, i.e., a linear approximation. First, as shown in Eq. (4),  $\theta$  is calibrated by minimizing the differences in sensitivities [1]. Assuming that there are a total of  $N+1$  training points,

$$\min_{\theta} \sum_{i=1}^N [\{y_{test}(d_{i+1}) - y_{test}(d_i)\} - \{y_{pre}(d_{i+1}, \theta) - y_{pre}(d_i, \theta)\}]^2 \quad (4)$$

In a multidimensional problem, the index  $i$  can be assigned to training points in such a way that two closest points have successive indices. Using the parameter  $\theta^*$  obtained by Eq. (4), the model discrepancy  $\delta$  can be obtained by Eq. (5) [1].

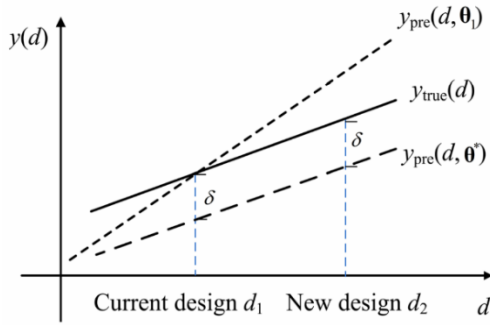


Fig. 2. Illustration of sensitivity based calibration method [1].

$$\min_{\delta} \sum_{i=1}^N [y_{test}(d_i) - y_{pre}(d_i, \theta^*) - \delta]^2 \quad (5)$$

The SLS matches the slope between two design points instead of directly matching the actual value and the simulation result. As shown in Fig. 2,  $\theta_1$  obtained from the conventional method, the FLS agrees well at the training point  $d_1$ , but does not properly follow the trend of the actual value, and an error occurs at the validation point  $d_2$  [1]. On the other hand,  $\theta^*$  obtained by the SLS did not coincide with the actual value, but the parameter was calibrated by capturing the trend of the actual value.

The goal of the SLS is to minimize the difference between the slope of the actual value and the slope of the simulation result. Therefore, to use the SLS, at least two training points are required, and to consider the discrepancy, the discrepancy is assumed in the form of the simplest constant function.

### 3. Example 1: I beam

In this section, the performances of the FLS and the SLS are compared using an I-beam example shown in Fig. 3. The objective function is the deflection at the tip of the beam and the design variable is the height of the beam. The calibration parameter is Young's modulus.

In the previous section, model prediction parameter was calibrated using test measurement. However, it is also possible to use a model with higher fidelity instead of measurement. In the I-beam example, Euler beam theory was used as a low-fidelity model which needs parameter calibration, while Timoshenko beam theory was used as a high-fidelity model. Both high- and low-fidelity models are implemented using finite element analysis software ANSYS.

As for the low-fidelity model, an I-beam was modeled in 1D as shown in Fig. 4 using the Euler theory, and a fixed support condition was applied at the base, and a force of 60 N was applied at the tip in the vertical direction to the ground. As a result of the simulation, the maximum deflection at the tip of the beam was 1.0603 mm. The goal is to calibrate the Young's modulus of the low-fidelity beam model so that the performance variable, the tip deflection is predicted with the minimum error compared to the high fidelity model in the whole design

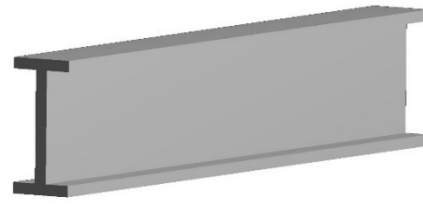


Fig. 3. I beam model.

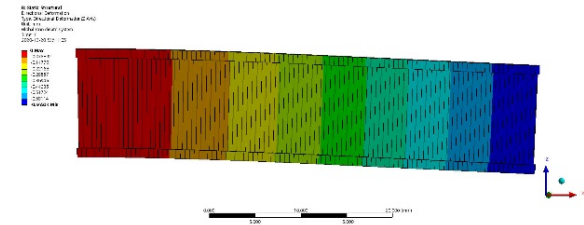


Fig. 4. Simulation of I beam based on Euler theory using ANSYS.

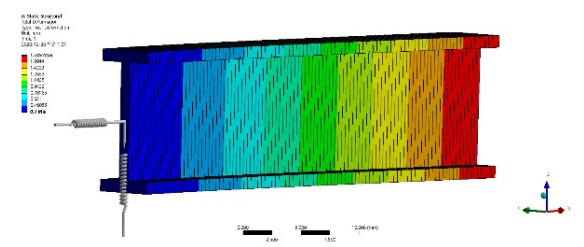


Fig. 5. Simulation of I beam based on Timoshenko theory using ANSYS.

domain.

To induce artificial model error, which seems plausible in real situations, it is assumed that the fixed boundary condition on the wall is not perfect in the high-fidelity model. Instead, the test condition was modeled with a longitudinal spring and a torsional spring on one base as shown in Fig. 5, and a force of 60 N was applied at the tip in the vertical direction to the ground. The stiffness of the spring was arbitrarily determined as 5.e+006 N/mm for the horizontal spring and 1.e+004 N/mm for the vertical one. The actual Young's modulus of the beam is 200 GPa.

The range of Young's modulus was set to 190000 MPa  $\leq E \leq$  209000 MPa, and the simulations were performed by an increment of 1000. When the beam height  $h$  was 8, 10, and 12, the tip deflection value  $y(h, E)$  according to the change of Young's modulus was calculated. These data were interpolated with a quadratic function using a MATLAB program to obtain Eqs. (6)-(8).

$$y(8, E) = 4.521 \times 10^{-11} E^2 - 2.707 \times 10^{-5} E + 5.401 \quad (6)$$

$$y(10, E) = 2.653 \times 10^{-11} E^2 - 1.592 \times 10^{-5} E + 3.184 \quad (7)$$

$$y(12, E) = 1.754 \times 10^{-11} E^2 - 1.049 \times 10^{-5} E + 2.092 \quad (8)$$

Using Eqs. (6)-(8) as true relationship between Young's modulus and tip deflection, Young's modulus in Euler beam

Table 1. Comparison of calibration accuracy for Young's modulus.

N (data point)	2 ( $h_i = 8, 10$ )		3 ( $h_i = 8, 10, 12$ )	
Method	FLS	SLS	FLS	SLS
E (MPa)	106370	199860	98083	199990
$\delta$	-	1.0483	-	1.0493

model was calculated by two calibration methods and the results are summarized in Table 1.

With the calibrated Young's modulus in Table 1, the tip deflection of the I-beam can be plotted as a function of design variable, the beam height,  $h$ . Fig. 6 shows the tip deflection curves using Young's modulus obtained from four different calibrations. The blue dashed curve (FLS2) represents the tip deflection curve of FLS obtained from two design points ( $h_i = 8, 10$ ), while the blue asterisked markers (FLS3) are obtained from three design points ( $h_i = 8, 10, 12$ ). Compared to the red-colored true curve, the prediction is only accurate at  $h = 9.5$  (FLS2) and  $h = 10$  (FLS3), but the prediction is inaccurate at other design points. It is also noted that  $h = 8$  and  $h = 12$  are used for calibration, but the predictions at these designs are not accurate. This happens because the calibration process tried to compensate for the model error.

On the other hand, the SLS methods in Fig. 6 do not match the red-colored true curve, but they follow the same trend with the true curve. This is expected because the SLS method minimizes the error in slope, not in the prediction. It is noted that the calibration using two designs are almost identical with that of three designs. This is expected because the calibrated Young's modulus in Table 1 was 199860 MPa for the two designs, and 199990 MPa for the three designs. Therefore, SLS is insensitive to the number of design points in this example.

Once Young's modulus was calibrated using the SLS methods, Eq. (5) was used to find the discrepancy  $\delta$ . It turns out that the constant discrepancy was 1.0483 mm. Once this discrepancy was incorporated with the prediction, Fig. 7 shows that the tip deflections using the SLS methods overlapped with the true curve.

In this section, the performance of the FLS and the SLS was compared through the example of I beam. It was confirmed that the FLS coincides at the training point, but the error increases as the validation point is further away from the training points. However, since the SLS captures and follows the trend of the actual model, there is little error even if the validation point moves away from the training point. Therefore, it can be clearly seen that the SLS is superior to the FLS in this example.

## 4. Example 2: open hole tension test

### 4.1 Open hole tension test

Tensile testing of perforated plates [13] was used to determine the effect of holes on tensile fracture strength in perforated specimens. The shape of the composite laminate speci-

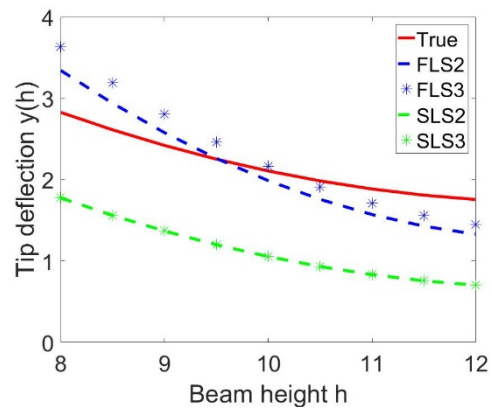


Fig. 6. Comparison of the results at I beam example from true model, FLS and SLS not including model discrepancy.

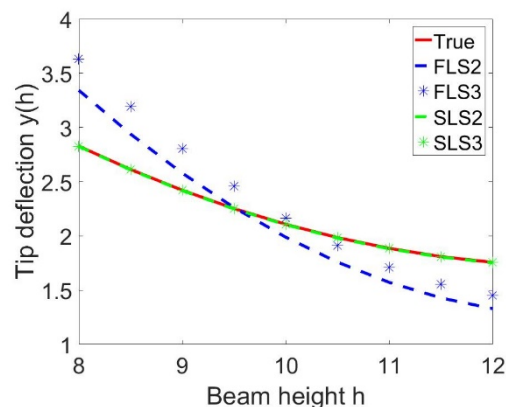


Fig. 7. Comparison of the results at I beam example from true model, FLS and SLS including model discrepancy.

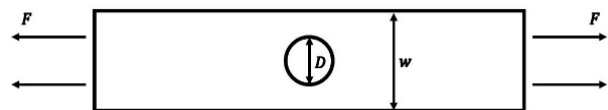


Fig. 8. Open hole tension test specimen.

men used in the experiments is shown in Fig. 8. Specimens were made of three distinct material batches. Force  $F$  was applied to both ends of the plate. The width of the specimen and the diameter of the hole are denoted by  $w$  and  $D$ , respectively. In this experiment, two control parameters were set. The first parameter is  $w/D$ , and  $w$  is changed as shown in Table 2. The second parameter  $N_{45}$  represents the different layups quantified by the fraction of  $\pm 45^\circ$  plies of the composite laminate and is changed as shown in Table 3. Each configuration consists of three prepreg batches, and each batch was repeated six times. The objective function is failure strength and the control variables are  $w/D$  and  $N_{45}$ . The calibration parameter is the characteristic length that is used in the Whitney-Nuismer model [14] which is used to predict the failure strength of laminate plates with a hole.

Table 2. w/D test matrix.

W (inch)	D (inch)	w/D	Batches/replicates	No. of specimens
0.75	0.250	3	3x6	18
1.00	0.250	4	3x6	18
1.50	0.250	6	3x6	18
2.00	0.250	8	3x6	18

Table 3. Layup test matrix.

N45	Layup % 0°/45°/90°	Ply stacking sequence	Batches/replicates	No. of specimens
0.2	40/20/40	[0/90/0/90/45/-45/90/0/90/0] <sub>5</sub>	3x6	18
0.5	25/50/25	[(45/0/-45/90) <sub>2</sub> ] <sub>5</sub>	3x6	18
0.8	10/80/10	[45/-45/90/45/-45/45/-45/0/45/-45] <sub>5</sub>	3x6	18

### 4.2 Whitney nuismer model

The tensile and compressive strength of a composite laminate with holes drops significantly as the hole diameter increases. Using the classical stress concentration factor, this drop cannot be accurately predicted. Therefore, Whitney and Nuismer hypothesized that the failure of a hole in an infinite plate under tension or compression can be determined when the stress at a certain characteristic distance away from the edge of the hole reaches the strength of the material without the hole [14].

Using the Whitney-Nuismer model, when there are circular holes in an isotropic plate, the stress failure criterion can be obtained as shown in Eq. (9).

$$\frac{\sigma_N}{\sigma_0} = \frac{2}{(2 + \xi^2 + 3\xi^4)}, \quad \xi = \frac{R}{R + d_0} \tag{9}$$

where  $\sigma_N$  is the strength of the laminate with holes and  $\sigma_0$  is the strength of the laminate without holes. Also,  $R$  is the radius of the hole and  $d_0$  is the characteristic distance.

In this work, the strain and stress of the tensile specimen with holes were obtained using the finite element program ABAQUS. The simulation was performed 42 times with a combination of  $w/D$  of 3, 4, 5, 6, 7, 8 and  $N_{45}$  of 0.2, 0.3, 0.4, 0.5, 0.6, 0.7, 0.8.

In Eq. (9),  $\sigma_0$  was obtained by finite element analysis of composite laminates without holes.

### 4.3 Calibration using two calibration factors

The experiment and simulation were combined as in Eq. (10) to fit the Whitney and Nuismer characteristic distances as a function of ( $w/D, N_{45}$ ).

$$d_0(w/D, N_{45}) = x_0 + x_1 N_{45} + x_2 w/D \tag{10}$$

Table 4. Averages of experimental strength  $\sigma_N$ .

Points	1	2	3	4	5	6
(w/D, N45)	(3, 0.2)	(4, 0.2)	(6, 0.2)	(8, 0.2)	(6, 0.5)	(6, 0.8)
$\sigma_N$	59.60	63.20	66.50	69.30	54.50	41.10

Table 5. Characteristic distance at experimental points.

w/D, N45	(3, 0.2)	(4, 0.2)	(6, 0.2)	(8, 0.2)	(6, 0.5)	(6, 0.8)
$d_0$ (inch)	0.044	0.052	0.060	0.067	0.063	0.094

Table 6. Comparison of the experimental value and the prediction value of  $\sigma_N$  using six data points.

Points (w/D, N45)	(3, 0.2)	(4, 0.2)	(6, 0.2)	(8, 0.2)	(6, 0.5)	(6, 0.8)
Experimental	59.60	63.20	66.50	69.30	54.50	41.10
Prediction	60.23	62.18	65.81	69.10	57.10	40.08
Error (%)	1.05	1.64	1.05	0.29	4.55	2.54

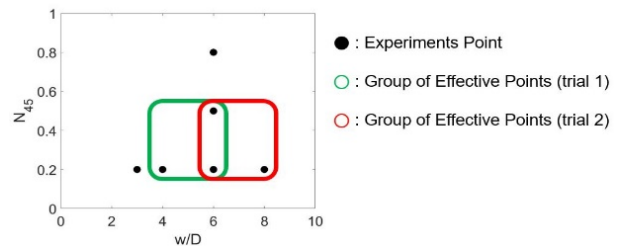


Fig. 9. Overview of effective points under calibration (trial 1, trial 2).

where  $x_0, x_1,$  and  $x_2$  are calibration parameters.

From the test matrices of  $w/D$  and  $N_{45}$ , six data points were generated as in Fig. 9 and the test results for  $\sigma_N$  are summarized in Table 4. The values are the average values calculated at each experimental point. The characteristic distance  $d_0$  from the origin can be calculated by Eq. (9) at each point, and the results are summarized in Table 5. Then, Eq. (10) is fitted using FLS as in Eq. (11).

$$d_{0\_ref}(w/D, N_{45}) = 0.0228 + 0.0484N_{45} + 0.0042w/D \tag{11}$$

Using Eqs. (9) and (11), the predicted values of  $\sigma_N$  at six data points were calculated and compared with the experimental values as in Table 6. This model is used as a reference to compare the performances of FLS and SLS calibrated with a smaller number of data points with model form error.

As shown in Fig. 9, two sets of three data points were chosen for the model calibration. For comparison purpose, two models were assumed, one with relatively small error (Eq. (12)) and the other with relatively bigger error (Eq. (13)). The purpose of this comparison was to demonstrate the capability of SLS to capture the trend of calibrated function while minimizing error caused by inaccuracy of model.

Table 7. Discrepancy in the prediction of  $\sigma_N$  from experimental data.

	(w/D, N45)	(3, 0.2)	(4, 0.2)	(6, 0.2)	(8, 0.2)	(6, 0.5)	(6, 0.8)
1	FLS (accurate)	0.34	2.46	0.93	0.50	0.18	10.63
	FLS (inaccurate)	10.13	9.15	2.86	1.48	0.42	8.59
	SLS (accurate)	3.84	0.58	0.08	0.03	0.07	11.81
	SLS (inaccurate)	3.84	0.58	0.08	0.03	0.07	11.81
2	FLS (accurate)	0.08	1.56	0.64	2.45	0.33	11.81
	FLS (inaccurate)	8.34	5.81	2.00	6.77	0.98	11.81
	SLS (accurate)	2.96	0.00	0.06	0.39	0.06	11.84
	SLS (inaccurate)	2.96	0.00	0.06	0.39	0.06	11.84

Table 8. RMSE results from FLS and SLS.

Points (w/D, N45)	RMSE
FLS (accurate)	1.859
FLS (inaccurate)	3.535
SLS (accurate)	1.978
SLS (inaccurate)	1.978

$$d_{\text{accurate}}(w/D, N_{45}) = 0.025 + x_1 N_{45} + x_2 w/D \quad (12)$$

$$d_{\text{inaccurate}}(w/D, N_{45}) = 0.005 + x_1 N_{45} + x_2 w/D \quad (13)$$

#### 4.3.1 Comparison of results based on model accuracy

The calibration parameters,  $x_1$ , and  $x_2$  were found by SLS and FLS, respectively, and the results of  $\sigma_N$  prediction are summarized in Table 7. It shows the error in the prediction by SLS and FLS deviated from the test results.

The root mean square error (RMSE) of  $\sigma_N$  calculated at all six data points and two sampling cases is summarized in Table 8. It is observed that the performance of the FLS and the SLS is similar if there exists a negligible model error. However, in the case of the FLS, the error increased as the model became inaccurate, and in the case of the SLS, the error was kept constant regardless of the accuracy of the model. Thus, it can be said that the model calibration using the sensitivity data augmented by the model discrepancy correction is more robust to the existence of model error than the conventional FLS.

#### 4.3.2 Function value based least squares method comparison based on model discrepancy considerations

To use the FLS regardless of the accuracy of the model, the model discrepancy  $\delta$  was considered like the SLS in the FLS. First, to assume that the model is accurate,  $\delta$  was added to

Table 9. RMSE results from FLS and FLS that considers model discrepancy.

Points (w/D, N45)	RMSE
FLS (accurate)	1.859
FLS+ $\delta$ (accurate)	1.976
FLS (inaccurate)	3.535
FLS+ $\delta$ (inaccurate)	1.980

Table 10. RMSE results from FLS that considers model discrepancy and SLS.

Points (w/D, N45)	RMSE
FLS+ $\delta$ (accurate)	1.976
SLS (accurate)	1.978
FLS+ $\delta$ (inaccurate)	1.980
SLS (inaccurate)	1.978

Eq. (12) and changed to Eq. (14).

$$d_0^{(1)}(w/D, N_{45}) = 0.025 + x_1 N_{45} + x_2 w/D + \delta, \quad (14)$$

The RMSE of the experimental and predicted values of the FLS and the FLS considering  $\delta$  was calculated as shown in Table 9. When the model is accurate, the error is similar regardless of whether  $\delta$  is present, but when the model is inaccurate, it can be seen that the error of the FLS taking  $\delta$  into account is significantly reduced.

The RMSE of the experimental and predicted values of the FLS considering  $\delta$  and the SLS was calculated as shown in Table 10. Regardless of the accuracy of the model, if  $\delta$  is considered in the FLS, there is little difference from the SLS. This is an expected result because a model error in the form of constant is assumed in this example. The performance of SLS with more complicated error form is to be investigated in our future research.

## 5. Conclusions

The performance and applicability of SLS method was investigated as a method for calibrating model parameters. To examine the performance of the SLS method, it was compared with that of an existing method, FLS, using two examples. The findings are as follows:

1) The SLS captures the trend of the actual value well, and when the model bias is obtained and removed, it almost coincides with the actual value at all points.

2) When the model is accurate, FLS and SLS perform similarly but SLS outperforms FLS as the model error increases. SLS shows more robust performance against the model errors.

3) SLS can be applied to multi-dimensional problems. However, a sophisticated logic needs to be developed to determine the order of training points in the multi-dimensional design space.

4) If the model error is constant, the FLS can be compensated by adding a bias in the model to be calibrated, and with this, the performance of FLS can become similar to that of SLS. The performance of SLS and FLS under more complicated form of model error needs to be investigated.

In most engineering simulation models, there are several model discrepancies, such as numerical and measurement errors. Thus, the SLS method investigated in this study would be a better choice when calibrating model parameters. If the FLS method is used, model bias  $\delta$  should be taken into account to yield more accurate results. In this paper, we used the FLS and the SLS through simple examples. However, if applied to more complex applications, more accurate calibration and validation would be possible if model discrepancy was considered by using a higher-order function rather than a constant. If the parameters are correctly calibrated and validated, it will be very helpful in reducing the number of unnecessary experiments and thus saving the experiment cost and time.

## Acknowledgments

This research was supported by the MOTIE (Ministry of Trade, Industry, and Energy) in Korea, under the Fostering Global Talents for Innovative Growth Program (P0008751) supervised by the Korea Institute for Advancement of Technology (KIAT).

## References

- [1] N. Qiu, C. Park, Y. Gao, J. Fang, G. Sun and N. H. Kim, Sensitivity-based parameter calibration and model validation under model error, *J. of Mechanical Design*, 140 (1) (2018) 011403.
- [2] J. A. Benek, E. M. Kraft and R. F. Lauer, Validation Issues for engine-airframe integration, *AIAA J.*, 36 (5) (1998) 759-764.
- [3] Z. Zhan, Y. Fu, R. J. Yang and Y. Peng, An automatic model calibration method for occupant restraint systems, *Structural and Multidisciplinary Optimization*, 44 (6) (2011) 815-822.
- [4] B. C. Jung, H. Yoon, H. Oh, G. Lee, M. Yoo, B. D. Youn and Y. C. Huh, Hierarchical model calibration for designing piezoelectric energy harvester in the presence of variability in material properties and geometry, *Structural and Multidisciplinary Optimization*, 53 (1) (2016) 161-173.
- [5] S. Sankararaman and S. Mahadevan, Integration of model verification, validation, and calibration for uncertainty quantification in engineering systems, *Reliability Engineering & System Safety*, 138 (2015) 194-209.
- [6] A. Borg, B. P. Husted and O. Njå, The concept of validation of numerical models for consequence analysis, *Reliability Engineering & System Safety*, 125 (2014) 36-45.
- [7] J. T. Oden, E. E. Prudencio and P. T. Bauman, Virtual model validation of complex multiscale systems: applications to nonlinear elastostatics, *Computer Methods in Applied Mechanics and Engineering*, 266 (2013) 162-184.
- [8] J. Loeppky, D. Bingham and W. Welch, *Computer Model Calibration or Tuning in Practice*, University of British Columbia, Vancouver, BC, Canada (2006).
- [9] M. C. Kennedy and A. O'Hagan, Bayesian calibration of computer models, *J. of the Royal Statistical Society, Series B: Statistical Methodology*, 63 (3) (2001) 425-464.
- [10] S. Zhang, P. Zhu, W. Chen and P. Arendt, Concurrent treatment of parametric uncertainty and metamodeling uncertainty in robust design, *Structural and Multidisciplinary Optimization*, 47 (1) (2013) 63-76.
- [11] Y. Ling, J. Mullins and S. Mahadevan, Selection of model discrepancy priors in Bayesian calibration, *J. of Computational Physics*, 276 (2014) 665-680.
- [12] L. E. Lindgren, H. Alberg and K. Domkin, Constitutive modeling and parameter optimisation, *International Conference on Computational Plasticity: 07/04/2003-10/04/2003. International Center for Numerical Methods in Engineering (CIMNE)* (2003).
- [13] Y. Zhang, J. Meeker, J. Schutte, N. Kim and R. Haftka, On approaches to combine experimental strength and simulation with application to open-hole-tension configuration, *Proc. of the American Society for Composites: Thirty-First Technical Conference*, Williamsburg, VA, USA (2016).
- [14] J. M. Whitney and R. J. Nuismer, Stress fracture criteria for laminated composites containing stress concentrations, *J. of Composite Materials*, 8 (3) (1974) 253-265.



**Gwangtaeck Lee** received his Bachelor's and Master's in Mechanical Engineering from Keimyung University, Daegu, Korea. His research interests include optimal design and dynamic impact simulation.



**Sanghoon Lee** is an Assistant Professor of Mechanical and Automotive Engineering at the Keimyung University, Daegu, South Korea. His Ph.D. in Mechanical Engineering is from Korea Advanced Institute of Science and Technology in 2006. His research area is design optimization, design under uncertainty, and radioactive waste package design and safety evaluation.



**Nam-Ho Kim** is presently Professor of Mechanical and Aerospace Engineering at the University of Florida. He graduated with a Ph.D. in Mechanical Engineering from the University of Iowa in 1999. His research area is structural design optimization, design sensitivity analysis, design under uncertainty, structural health monitoring, nonlinear structural mechanics, and structural-acoustics.